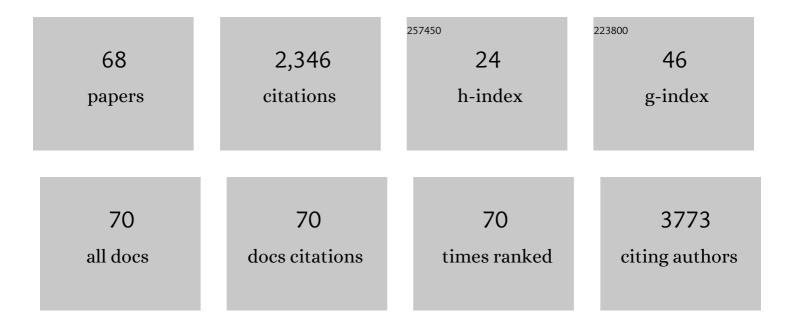
Yuying Zhang

List of Publications by Year in descending order

Source: https://exaly.com/author-pdf/6742684/publications.pdf Version: 2024-02-01



#	Article	IF	CITATIONS
1	Physicochemical characterization and antioxidant activity of quercetinâ€loaded chitosan nanoparticles. Journal of Applied Polymer Science, 2008, 107, 891-897.	2.6	218
2	Poly(lactide-co-glycolide)/hydroxyapatite nanofibrous scaffolds fabricated by electrospinning for bone tissue engineering. Journal of Materials Science: Materials in Medicine, 2011, 22, 1873-1884.	3.6	156
3	A Mitochondrial-Targeting Near-Infrared Fluorescent Probe for Visualizing and Monitoring Viscosity in Live Cells and Tissues. Analytical Chemistry, 2019, 91, 10302-10309.	6.5	154
4	Legumain promotes tubular ferroptosis by facilitating chaperone-mediated autophagy of GPX4 in AKI. Cell Death and Disease, 2021, 12, 65.	6.3	143
5	Recent Progress on Liquid Biopsy Analysis using Surface-Enhanced Raman Spectroscopy. Theranostics, 2019, 9, 491-525.	10.0	114
6	Nuclear Targeted Nanoprobe for Single Living Cell Detection by Surface-Enhanced Raman Scattering. Bioconjugate Chemistry, 2009, 20, 768-773.	3.6	112
7	Salmonella enterica Remodels the Host Cell Endosomal System for Efficient Intravacuolar Nutrition. Cell Host and Microbe, 2017, 21, 390-402.	11.0	109
8	Influence of silica particle internalization on adhesion and migration of human dermal fibroblasts. Biomaterials, 2010, 31, 8465-8474.	11.4	106
9	Transport of a Cancer Chemopreventive Polyphenol, Resveratrol: Interaction with Serum Albumin and Hemoglobin. Journal of Fluorescence, 2007, 17, 580-587.	2.5	104
10	Lighting Up NIR-II Fluorescence in Vivo: An Activable Probe for Noninvasive Hydroxyl Radical Imaging. Analytical Chemistry, 2019, 91, 15757-15762.	6.5	88
11	Cancer-derived exosomal miR-138-5p modulates polarization of tumor-associated macrophages through inhibition of KDM6B. Theranostics, 2021, 11, 6847-6859.	10.0	77
12	Toxicity of ZnO Nanoparticles to Macrophages Due to Cell Uptake and Intracellular Release of Zinc Ions. Journal of Nanoscience and Nanotechnology, 2014, 14, 5688-5696.	0.9	76
13	Gold and silver nanoparticle monomers are non-SERS-active: a negative experimental study with silica-encapsulated Raman-reporter-coated metal colloids. Physical Chemistry Chemical Physics, 2015, 17, 21120-21126.	2.8	76
14	Reorganization of the Endosomal System in Salmonella-Infected Cells: The Ultrastructure of Salmonella-Induced Tubular Compartments. PLoS Pathogens, 2014, 10, e1004374.	4.7	64
15	Influence of Surface Coating of PLGA Particles on the Internalization and Functions of Human Endothelial Cells. Biomacromolecules, 2012, 13, 3272-3282.	5.4	53
16	KRAS(G12D) can be targeted by potent inhibitors via formation of salt bridge. Cell Discovery, 2022, 8, 5.	6.7	52
17	Influences of Acid-Treated Multiwalled Carbon Nanotubes on Fibroblasts: Proliferation, Adhesion, Migration, and Wound Healing. Annals of Biomedical Engineering, 2011, 39, 414-426.	2.5	46
18	Interaction of the docetaxel with human serum albumin using optical spectroscopy methods. Journal of Luminescence, 2009, 129, 1196-1203.	3.1	39

YUYING ZHANG

#	Article	IF	CITATIONS
19	Cellular Uptake of Covalent Poly(allylamine hydrochloride) Microcapsules and Its Influences on Cell Functions. Macromolecular Bioscience, 2012, 12, 1534-1545.	4.1	37
20	Influences of surface chemistry and swelling of salt-treated polyelectrolyte multilayers on migration of smooth muscle cells. Journal of the Royal Society Interface, 2012, 9, 3455-3468.	3.4	34
21	Evaluation of nanoparticles as endocytic tracers in cellular microbiology. Nanoscale, 2013, 5, 9296.	5.6	32
22	Cryo-EM structure of <i>Mycobacterium smegmatis</i> DyP-loaded encapsulin. Proceedings of the National Academy of Sciences of the United States of America, 2021, 118, .	7.1	32
23	Etchable SERS nanosensor for accurate pH and hydrogen peroxide sensing in living cells. Chemical Communications, 2019, 55, 12996-12999.	4.1	29
24	Effect of Antigen Retrieval Methods on Nonspecific Binding of Antibody–Metal Nanoparticle Conjugates on Formalin-Fixed Paraffin-Embedded Tissue. Analytical Chemistry, 2018, 90, 760-768.	6.5	28
25	Cryo-EM structure of mycobacterial cytochrome bd reveals two oxygen access channels. Nature Communications, 2021, 12, 4621.	12.8	24
26	Preparation and cellular uptake of PLGA particles loaded with lamivudine. Science Bulletin, 2012, 57, 3985-3993.	1.7	22
27	Structure of Mycobacterium tuberculosis cytochrome bcc in complex with Q203 and TB47, two anti-TB drug candidates. ELife, 2021, 10, .	6.0	22
28	Cryo-EM structure of trimeric Mycobacterium smegmatis succinate dehydrogenase with a membrane-anchor SdhF. Nature Communications, 2020, 11, 4245.	12.8	20
29	Study of the Selective Uptake Progress of Aptamerâ€ <scp>M</scp> odified <scp>PLGA</scp> Particles by Liver Cells. Macromolecular Bioscience, 2013, 13, 1413-1421.	4.1	19
30	Legumain-deficient macrophages promote senescence of tumor cells by sustaining JAK1/STAT1 activation. Cancer Letters, 2020, 472, 40-49.	7.2	18
31	Stimulus-responsive surface-enhanced Raman scattering: a "Trojan horse―strategy for precision molecular diagnosis of cancer. Chemical Science, 2020, 11, 6111-6120.	7.4	17
32	Solution properties of water-insoluble polysaccharides from the mycelium of Ganoderma tsugae. Carbohydrate Polymers, 2005, 59, 351-356.	10.2	16
33	Encapsulation of Photosensitizer into Multilayer Microcapsules by Combination of Spontaneous Deposition and Heatâ€Induced Shrinkage for Photodynamic Therapy. Macromolecular Bioscience, 2012, 12, 1436-1442.	4.1	16
34	Mineralization of Collagenâ€Coated Electrospun Poly(lactideâ€ <i>co</i> â€glycolide) Nanofibrous Mesh to Enhance Growth and Differentiation of Osteoblasts and Bone Marrow Mesenchymal Stem Cells. Advanced Engineering Materials, 2012, 14, B123.	3.5	15
35	Asparagine endopeptidase-targeted Ultrasound-responsive Nanobubbles Alleviate Tau Cleavage and Amyloid-1² Deposition in an Alzheimer's Disease Model. Acta Biomaterialia, 2022, 141, 388-397.	8.3	15
36	Loss of legumain induces premature senescence and mediates agingâ€related renal fibrosis. Aging Cell, 2022, 21, e13574.	6.7	15

YUYING ZHANG

#	Article	IF	CITATIONS
37	iSERS microscopy guided by wide field immunofluorescence: analysis of HER2 expression on normal and breast cancer FFPE tissue sections. Analyst, The, 2016, 141, 5113-5119.	3.5	14
38	Plasmonic metal/semiconductor hybrid nanomaterials for solar to chemical energy conversion. Journal of Energy Chemistry, 2021, 63, 40-53.	12.9	13
39	Fabrication of Chitosan Singleâ€Component Microcapsules With a Micrometerâ€Thick and Layered Wall Structure by Stepwise Coreâ€Mediated Precipitation. Macromolecular Rapid Communications, 2012, 33, 326-331.	3.9	10
40	Asparaginyl endopeptidase induces endothelial permeability and tumor metastasis via downregulating zonula occludens protein ZO-1. Biochimica Et Biophysica Acta - Molecular Basis of Disease, 2019, 1865, 2267-2275.	3.8	9
41	ImmunoSERS microscopy for the detection of smooth muscle cells in atherosclerotic plaques. Biosensors and Bioelectronics, 2019, 133, 79-85.	10.1	9
42	Modified reduced graphene oxide as stabilizer for Pickering w/o emulsions. Journal of Materials Science, 2020, 55, 1946-1958.	3.7	9
43	Combined legumain- and integrin-targeted nanobubbles for molecular ultrasound imaging of breast cancer. Nanomedicine: Nanotechnology, Biology, and Medicine, 2022, 42, 102533.	3.3	9
44	Comparison of Chondrocytes in Knee Osteoarthritis and Regulation by Scaffold Pore Size and Stiffness. Tissue Engineering - Part A, 2021, 27, 223-236.	3.1	8
45	Synthesis, characterization and crystal structure of a novel three-dimensional supramolecular architecture formed by manganese(II) and pyridine-2,5-dicarboxylic acid. Journal of Coordination Chemistry, 2006, 59, 389-393.	2.2	6
46	pH Induces Thermal Unfolding of UTI: An Implication of Reversible and Irreversible Mechanism Based on the Analysis of Thermal Stability, Thermodynamic, Conformational Characterization. Journal of Fluorescence, 2008, 18, 305-317.	2.5	6
47	Influence of folate conjugation on the cellular uptake degree of poly(allylamine hydrochloride) microcapsules. Journal of Applied Polymer Science, 2011, 121, 3710-3716.	2.6	6
48	Alginate microspheres prepared by ionic crosslinking of pickering alginate emulsions. Journal of Biomaterials Science, Polymer Edition, 2019, 30, 1083-1096.	3.5	6
49	EFFECT OF CELLULAR UPTAKE OF SiO ₂ PARTICLES ON ADHESION AND MIGRATION OF HepG2 CELLS. Acta Polymerica Sinica, 2009, 009, 815-822.	0.0	5
50	Reproducible fabrication of gold nanostar monolayers for surfaceâ€enhanced Raman spectroscopyâ€based trace detection. Journal of Raman Spectroscopy, 2022, 53, 1227-1237.	2.5	5
51	Several Key Factors for Efficient Electrocatalytic Water Splitting: Active Site Coordination Environment, Morphology Changes and Intermediates Identification. Chemistry - A European Journal, 2022, 28, .	3.3	5
52	Colorimetric analysis of extracellular vesicle surface proteins based on controlled growth of Au aptasensors. Analyst, The, 2021, 146, 2019-2028.	3.5	4
53	Size-Dependent Penetration of Gold Nanoprobes into Fixed Cells. ACS Omega, 2021, 6, 3791-3799.	3.5	4
54	Synthesis, structure, and properties of a 1-D copper(II) complex with nitronyl nitroxide radicals. Journal of Coordination Chemistry, 2009, 62, 2076-2085.	2.2	3

YUYING ZHANG

#	Article	IF	CITATIONS
55	Preparation of Main-Chain Thermotropic Polyesters With Two Types of Mesogens Connected Alternatively by Aliphatic Spacers. Journal of Macromolecular Science - Physics, 2010, 50, 363-375.	1.0	3
56	Application of Fluorescent Nanoparticles to Study Remodeling of the Endo-lysosomal System by Intracellular Bacteria. Journal of Visualized Experiments, 2015, , e52058.	0.3	3
57	Immuno-SERS: from nanotag design to assays and microscopy. , 2020, , 485-528.		3
58	Urea/NaOH aqueous solution as new solvent of aeromonas gum. Journal of Applied Polymer Science, 2005, 97, 1710-1713.	2.6	2
59	Synthesis, Characterization and Crystal Structure of a Novel Three-Dimensional Supramolecular Architecture Formed by Cobalt(II) and Pyridine-2,5-dicarboxylic Acid. Synthesis and Reactivity in Inorganic, Metal Organic, and Nano Metal Chemistry, 2008, 38, 701-704.	0.6	2
60	A hydrogen-bonded, one-dimensional complex of cadmium(II) ions with 3,5-dinitrobenzoate and radicals: synthesis, characterization and crystal structure. Journal of Coordination Chemistry, 2006, 59, 325-331.	2.2	1
61	Interaction of daunomycin antibiotic with human α1-acid glycoprotein: Spectroscopy and modeling. Journal of Molecular Structure, 2006, 788, 30-35.	3.6	1
62	Influence of surface coatings of poly(<scp>d</scp> , <scp>l</scp> -lactide- <i>co</i> -glycolide) particles on HepG2 cell behavior and particle fate. Biointerphases, 2014, 9, 031015.	1.6	1
63	Synthetic liver fibrotic niche extracts achieve inÂvitro hepatoblasts phenotype enhancement and expansion. IScience, 2021, 24, 103303.	4.1	1
64	Synthesis, Crystal Structure and Magnetic Property of a Complex Containing Silver Ions with Thiazoleâ€substituted Nitronyl Nitroxide Radicals. Synthesis and Reactivity in Inorganic, Metal Organic, and Nano Metal Chemistry, 2007, 37, 199-201.	0.6	0
65	A Novel Ferromagnetic Coupling Complex with Silver Ion and Nitronyl Nitroxide. Synthesis and Reactivity in Inorganic, Metal Organic, and Nano Metal Chemistry, 2008, 38, 669-672.	0.6	0
66	Synthesis, crystal structure and magnetic properties of Co(NIT4Py)(H2PDA)(H2O)3. Journal of Coordination Chemistry, 2008, 61, 1797-1803.	2.2	0
67	iSERS microscopy: point-of-care diagnosis and tissue imaging. , 2022, , 327-372.		0
68	iSERS Microscopy for Cellular and Tissue Imaging <i>Ex Vivo</i> . , 2022, , 273-321.		0